Current Applied Physics 12 (2012) 597–601

Contents lists available at SciVerse ScienceDirect

Current Applied Physics

journal homepage: www.elsevier.com/locate/cap

Electrical and electroluminescence properties of ITO/PEDOT:PSS/TPD:Alq_3:C_{60}/Al organic light emitting diodes

Mina Neghabi[a], Abbas Behjat[a,b,*]

[a] Atomic and Molecular Group, Physics Department, Yazd University, Yazd, Iran
[b] Photonics Group, Engineering Research Center, Yazd University, Yazd, Iran

ARTICLE INFO

Article history:
Received 3 July 2011
Received in revised form
10 September 2011
Accepted 15 September 2011
Available online 28 September 2011

Keywords:
Organic light emitting diodes
Polymer blends
Mobility
Fullerene

ABSTRACT

Organic light emitting diodes (OLEDs) of ITO/PEDOT:PSS/TPD:Alq_3:C_{60}/Al with different C_{60} concentrations (0–6.0 wt.%) have been fabricated. The physical parameters including electrical and optical properties of the samples have been measured by Luminance–current–voltage (L–I–V) characteristics and optical absorbance. The current–voltage characteristics indicate that field-emission tunneling injection dominates in the diodes at high applied voltages. It is found that with increasing the concentration of C_{60}, the injection barrier for holes slightly reduces and the hole's mobility increases over two orders of magnitude. Also, electroluminescence enhances with the presence of C_{60} in the blend; optimum current efficiency occurs at 3 wt% C_{60}. The method provides a simple way of increasing the efficiency of OLEDs.

1. Introduction

In recent years, research on organic light emitting diodes (OLEDs) based on the blend of different electroactive materials have been significantly increased. This is because of their possible application in large scale lighting, flexible panel and multi color displays with low power consumption and low cost [1–4]. Charge injection, transport and recombination processes are important factors that can influence efficiency and electroluminescence properties of the devices [5–8]. Also, it has been well demonstrated that increase in the efficiency and lifetime of the device, strongly depends on decreasing of the charge's injection barriers at the interfaces and the charge balance in a controlled electron–hole recombination zone [9–11].

One way to obtain devices with high performance is utilizing the blend structure of solution-processible materials. In the blending technique one enables to incorporate the efficient charge transport organic materials into the device and also increase the device performance, by control of the concentration of blend materials [12–17].

In this paper, we study the optical and electrical characteristics of ITO/PEDOT:PSS/Blend (TPD:Alq_3:C_{60})/Al heterostructure devices with different C_{60} concentrations. Here, fullerene (C_{60}) has been used to increase the hole transport process in the TPD:Alq_3 blend. Also, a comprehensive study is carried out to understand mechanisms of charge carrier injection and transport for the devices by current–voltage and luminance–voltage characterization.

2. Experimental

N, N′-bis(3-methylphenyl)-N, N′-diphenylbenzidine (TPD), tris(8-hydroxyquinoline) aluminum (Alq_3), poly-3,4-ethylenedioxythiophene/polystyrenesulphonate (PEDOT:PSS) and fullerene (C_{60}) were purchased from Sigma-Aldrich and used as received. The ITO glasses having a sheet resistance of 15 Ω/sq were also purchased from Sigma-Aldrich. A 5-mm wide ITO anode strip line was made by selective etching; using mixed solutions of hydrochloric acid (HCl) and nitric acid (HNO_3) at a volume ratio of 3:1 for 10–20 min at room temperature. Then, the patterned anode glass was cleaned sequentially by ultra-sonication in propanol, acetone, deionized water for 10 min, respectively. Then the substrates were dried in a high purity N_2 gas stream. PEDOT:PSS as a hole injection layer was spin-coated onto the anodes and then dried in the oven at 110 °C for 1 h. The TPD and Alq_3 were dissolved in chloroform solution with a concentration of 15 mg/ml with 10:2 weight ratios. The C_{60} was dissolved in toluene and blended with TPD and Alq_3 with different concentrations (i.e. 0, 0.7, 1.5, 3, and 6% by weight). Then the blend was spin-coated onto the prepared substrate; anode

* Corresponding author. Photonics Group, Engineering Research Center, Yazd University, Pajouhesh Street, Yazd 89195-741, Iran. Tel.: +98 351 8122773; fax: +98 351 8200132.
E-mail address: abehjat@yazduni.ac.ir (A. Behjat).

1567-1739/$ – see front matter © 2011 Elsevier B.V. All rights reserved.
doi:10.1016/j.cap.2011.09.010

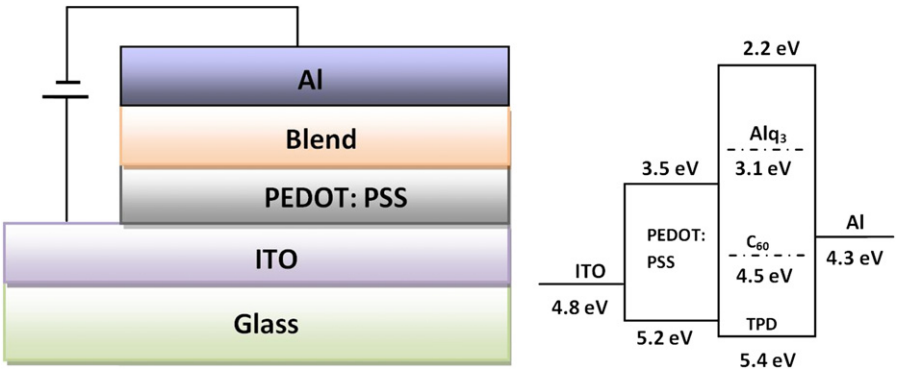

Fig. 1. Schematic device structure and band diagram of organic light emitting diode.

glass coated with PEDOT:PSS. The thicknesses of spin-coated layers were measured by means of Decktac 8000 profilmeter. Finally, the aluminum was deposited by thermal evaporation as a cathode at room temperature. The base pressure in the vacuum chamber was 10^{-3} Pa ($\sim 10^{-6}$ Torr) during the evaporation process. The Al was heated in tungsten boats. The film deposition rate was 0.1 nm/s. The thickness of the Al film was monitored in situ by a quartz crystal thickness measuring device. Fig. 1 shows a schematic diagram and band structure of the ITO/PEDOT:PSS/Blend/Al device.

The optical absorption spectra of the blends were obtained using Perkin–Elmer UV–VIS spectrometer. A Keithley 2400 source-meter and a JAZ spectrometer (Ocean optic) were used to record current–voltage and light–current characteristics of the devices, simultaneously.

3. Results and discussion

3.1. Absorption of blends

Fig. 2 shows the normalized optical absorption spectra of the TPD:Alq_3 and TPD:Alq_3:C_{60} blends. It can be seen that there are four major absorption peaks in UV–VIS regions. It has been reported that the absorption peak at about 357 nm is related to TPD [12] and the peaks centered at 268 and 390 nm are characteristic of Alq_3 [15]. So, the absorption spectrum of the blend is superposition of absorption spectra of the two components. Also, it has been found that for pristine C_{60}, the absorption spectrum has a peak at 330 nm which represents h_u-t_{1g} dipole-allowed electronic transition [18]. Therefore the TPD:Alq_3:C_{60} has an absorption peak at 330 nm compare with the TPD:Alq_3 blend.

3.2. Charge carrier injection

The current density–voltage characteristics of the ITO/PEDOT:PSS/TPD:Alq_3:C_{60}/Al with different C_{60} concentrations and the ITO/PEDOT:PSS/TPD:Alq_3/Al devices were measured and results were shown in Fig. 3. Two models are mainly used to describe charge carrier injection mechanism in OLED devices; the Richardson–Schottky (RS) thermionic emission and Fowler–Nordheim (FN) tunneling model [19]. In the RS model, tunneling is ignored and when charge carriers obtain sufficient thermal energy to overcome the maximum potential, resulting from the superposition of the external and the image–charge potential, then are injected from the contact. The temperature dependent current density is given by:

$$j_{RS} = A^* T^2 \exp\left[-\frac{\varphi_B}{k_B T}\right] \exp\left[\frac{\beta_{RS}\sqrt{F}}{k_B T}\right] \quad (1)$$

Here, $A^*$is the Richardson constant ($A^* = 120\ A/cm^2\ K^2$ if the effective mass of electrons inside the dielectric is equal to free

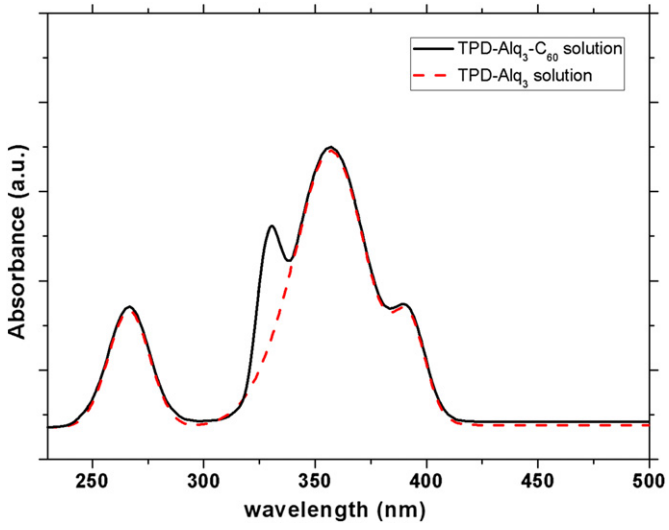

Fig. 2. The absorption spectra of the TPD:Alq_3 and TPD:Alq_3 doped with 0.7 wt% C_{60}.

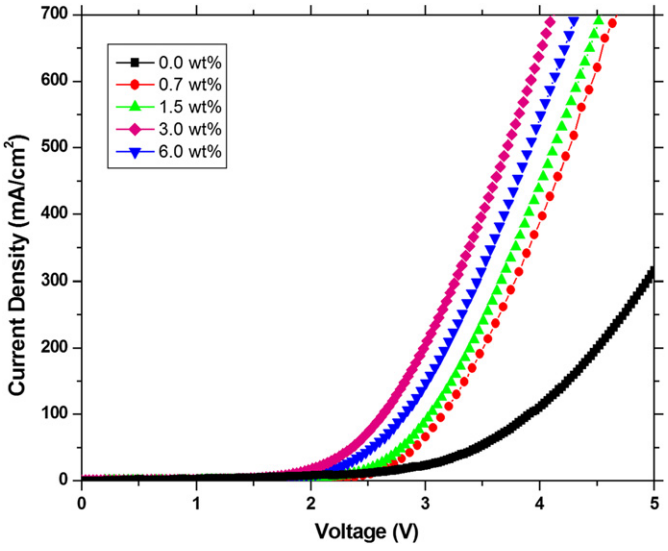

Fig. 3. J–V characteristics of OLEDs at different C_{60} concentrations.

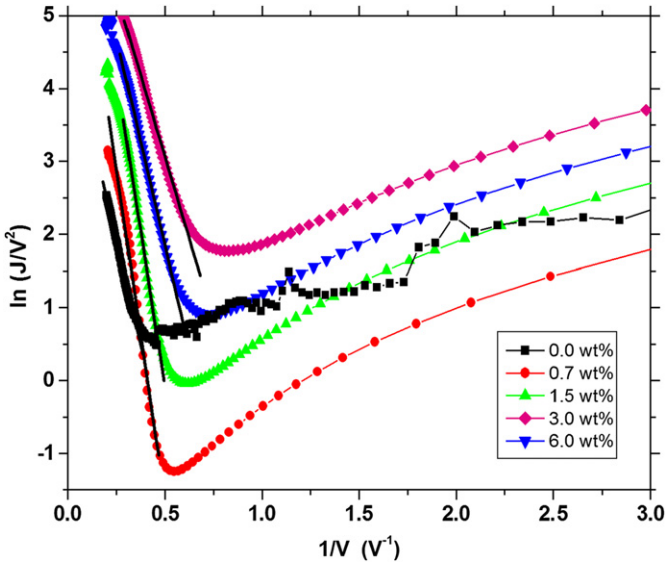

Fig. 4. Current density–voltage characteristics of OLEDs with different C_{60} concentration: Fowler–Nordheim type plot.

electron mass), T is the temperature in K, φ_B is the zero field barrier height, and F is the external electric field. According to the FN model, charge carriers are injected into the semiconductor by tunneling. Ignoring the image–charge effects and assuming tunneling through a triangular barrier, the FN model yields:

$$j_{FN} = \frac{q^3F^2}{8\pi h\varphi_B}\exp\left[\frac{8\pi(2m^*)^{1/2}\varphi_B^{2/3}}{3heF}\right] \quad (2)$$

Basically, the charge carrier injection mechanism into OLED devices is investigated by a RS type plot, $\log J$ vs. $V^{1/2}$ and a FN type plot, $\ln(J/V^2)$ vs. $1/V$. There is no linear dependence of the current density (J) versus the square root of the electric field ($V^{1/2}$) and also that there is no temperature and thickness dependence of I–V characteristic (not shown), indicating that the charge injection is due to the tunneling. As it can be seen from Fig. 4, all five curves at high voltage can be fit to a straight line and one can calculate the barrier height φ for the hole injection from the ITO electrode from the slope of FN plot. The barrier heights calculated for the various samples are presented in Table 1. It can be seen that the barrier height of the structures changes from 0.1 to 0.06 eV. The hole injection barrier height decreases with increasing concentration of C_{60}. It seems that when concentration of C_{60} increases, many electrons transfer from Alq_3 to C_{60} regarding to the strong electron-acceptance ability of C_{60}. So, the electrons could accumulate at the ITO/blend interface results in local electric field effect. Therefore, hole injection from ITO into blend film is favored and hole injection barrier height decreased.

Table 1
The hole mobility and barrier height at ITO/PEDOT:PSS/Blend/Al with different C_{60} concentrations in blend.

Blend	μ ($cm^2\ V^{-1}\ S^{-1}$)	Φ_B (eV)
(TPD:Alq_3)	$(9.5 \pm 0.5) \times 10^{-8}$	0.11
(TPD:Alq_3:C_{60}(0.7 wt%))	$(3.2 \pm 0.2) \times 10^{-7}$	0.10
(TPD:Alq_3:C_{60}(1.5 wt%))	$(4.9 \pm 0.3) \times 10^{-7}$	0.09
(TPD:Alq_3:C_{60}(3 wt%))	$(10 \pm 0.6) \times 10^{-7}$	0.06
(TPD:Alq_3:C_{60}(6 wt%))	$(7.7 \pm 0.4) \times 10^{-7}$	0.07

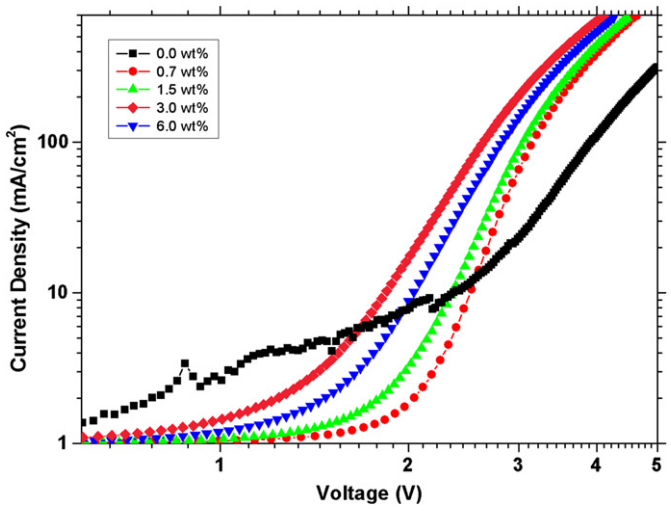

Fig. 5. Variation of the log J versus log V.

3.3. Charge carrier transport

The J–V characteristics of the devices were studied to understand the effects of C_{60} doping on the carrier transport and to illustrate transport limited mechanism. Fig. 5 shows that the current approximately obeys a power law of the form ($J \propto V^{m+1}$). There are three different voltage regions. In the first region, at low voltages, m approximately is zero ($J \propto V$) which indicates that charge carrier transport limited mechanism is Ohmic transport. In this case the contact, so-called "Ohmic" contact, can serve as an unlimited reservoir of charge carriers. In second region, that includes intermediate voltages, m varies between 9 and 5.3 for different C_{60} concentrations. This behavior could be described as an indication for trap charge limited conduction (TCLC). It was demonstrated that as the fraction of C_{60} increases, higher empirical parameter m is observed; which indicates that the density of trap states in band gap are decreased. According to Fig. 1, the lowest unoccupied molecular orbital (LUMO) of C_{60} in blended films is low enough to accept electrons from cathode. This character of C_{60} might increase

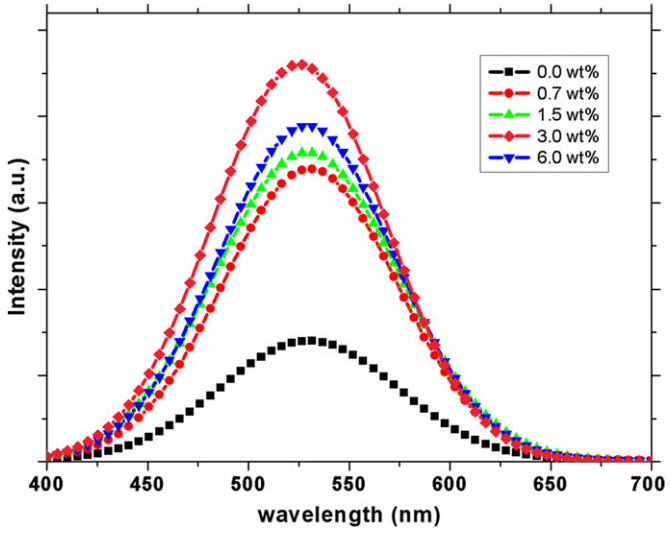

Fig. 6. EL spectra under a driving voltage of 10 V device structures: ITO/PEDOT:PSS/TPD:ALq_3:C_{60}/Al.

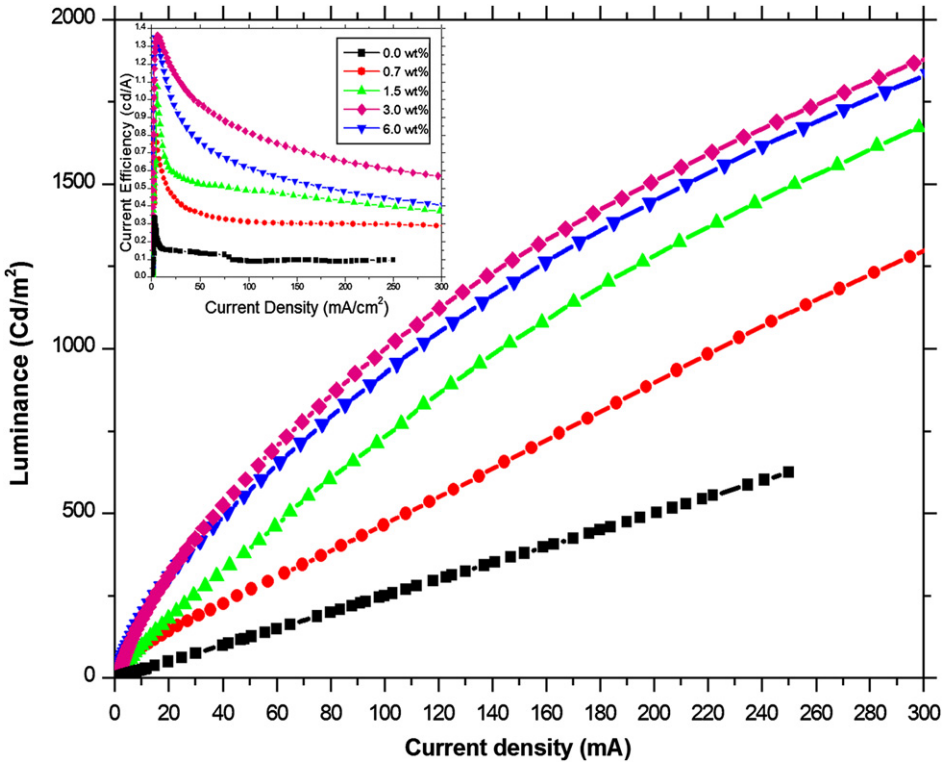

Fig. 7. The *L–V* characteristics of ITO/PEDOT:PSS/Blend/Al with different C_{60} Concentrations. The inset shows the current efficiency as a function of current density for ITO/PEDOT:PSS/Blend/Al with different C_{60} Concentrations.

electrons and the interchange hopping of positive carriers, which lead to more filling of traps in the blend films.

Third region, in Fig. 5 demonstrated $m \approx 2$ for all samples indicating that in this case, the current at high voltages is space charge limited (SCLC). Almost all traps are filled and therefore dependence of current and voltage obeys Child's law [20]:

$$j_{SCLC} = \frac{9}{8}\varepsilon\,\varepsilon_0\mu\,\frac{V^2}{d^3} \tag{3}$$

where ε is the relative dielectric constant, ε_0 the permittivity of vacuum, μ the effective charge carrier mobility, d the organic layer thickness and V is the applied voltage. Assuming $\varepsilon = 3$ [21], the charge carrier mobility in the blend films is calculated using equation (3) and are shown in Table 1. It can be seen that the hole mobility increases over two orders of magnitude with increasing C_{60} concentration. Presence of C_{60} in blend films, alter the relative positions of the LUMOs and might increase the interchain hopping of holes, which lead to high-hole mobility in the C_{60}-doped blend films and is in agreement with above expressions.

3.4. Photophysical properties

The electroluminescence (EL) spectra of C_{60}-doped blend devices along with the EL spectrum of device without C_{60} at 10 V bias are depicted in Fig. 6. It is obvious that the C_{60} concentration can strongly influence the EL intensity of the devices. The main emission is observed at 530 nm indicating that green light originating from Alq_3. The plots of luminance versus current density (*L–J*) of the samples are shown in Fig. 7. Current efficiency of blend films was calculated using the current density and luminance data. The current efficiency as a function of current density for ITO/PEDOT/Blend/Al devices with different concentrations of C_{60} is shown in the inset of Fig. 7. As it can be seen the EL intensity and the current efficiency of the devices are increased with increasing C_{60} concentration. These results are in good agreement with the previous research [22,23]. The improvement in EL intensity and current efficiency could be due to enhancement of hole injection and more balanced hole and electron fluxes. However, when C_{60} concentration in the blend film was increased to 6.0% by weight, EL intensity and current efficiency of the device were decreased indicating that more holes injection would cause the surface leakage current and create unbalance in hole and electron carriers that led to lower current efficiency in blend films.

4. Conclusion

In summary, the charge carrier injection and transport characteristics of TPD:Alq_3:C_{60} blends were studied. The *J–V* measurements showed that tunneling injection (FN model) dominates in high voltage regime and the hole injection barrier height decreases with increasing the concentration of C_{60} in the blend. It was found that the hole mobility in a TPD:Alq_3:C_{60} blend increases with increasing C_{60} content, which can be explained by increasing of the interchain hopping of holes in the blend films. Also, a significant increase of EL intensity and current efficiency was observed by increasing concentration of the C_{60} up to 3 wt%. This improvement is due to enhancement of the hole injection and more balance in hole and electron fluxes. The method provides a simple way in order to increase the efficiency of OLEDs.

Acknowledgments

The support of the Ministry of Energy for this project is gratefully acknowledged. Authors also wish to thank the photonics group of Physics Department, Yazd University for Laboratory support.

References

[1] P. Kopola, M. Tuomikoski, R. Suhonen, A. Maaninen, Thin Solid Films 517 (2009) 5757–5762.
[2] R. Bathelt, D. Buchhauser, C. Gärditz, R. Paetzold, P. Wellmann, Org. Electron. 8 (2007) 293–299.
[3] A.R. Duggal, C.M. Heller, J.J. Shiang, J. Liu, L.N. Lewis, J. Display Technol. 3 (2007) 184–192.
[4] S.A. Choulis, Vi-En Choong, M.K. Mathai, F. So, Appl. Phys. Lett. 87 (2005) 11350–11353.
[5] M.B. Khalifa, D. Vaufrey, J. Tardy, Org. Electron. 5 (2004) 187–198.
[6] M.B. Khalifa, D. Vaufrey, A. Bouazizi, J. Tardy, H. Maaref, Mater. Sci. Eng. C 21 (2002) 277–282.
[7] S.L.M. van Mensfoort, R.J. de Vries, V. Shabro, H.P. Loebl, R.A.J. Janssen, R. Coehoorn, Org. Electron. 11 (2010) 1408–1413.
[8] P. D'Angelo, M. Barra, A. Cassinese, M.G. Maglione, P. Vacca, C. Minarini, A. Rubino, Solid State Electron. 51 (2007) 123–129.
[9] Y.H. Lee, W.J. Kim, T.Y. Kim, J. Jung, J.Y. Lee, H.D. Park, T.W. Kim, J.W. Hong, Curr. Appl. Phys. 7 (2007) 409–412.
[10] Q. Sun, X. Zhan, C. Yang, Y. Liu, Y. Li, D. Zhu, Thin Solid Films 440 (2003) 247–254.
[11] B. Mazhari, Solid State Electron. 49 (2005) 311–315.
[12] N.S. Eremina, L.G. Samsonova, T.N. Kopylova, G.V. Mayer, K.M. Degtyarenko, E.N. Tel'minov, R.M. Gadirov, A.V. Mesentseva, Russ. Phys. J. 51 (2008) 536–543.
[13] P.K. Nayaka, N. Agarwala, N. Periasamy, M.P. Patankar, K.L. Narasimhan, Synth. Met. 160 (2010) 722–727.
[14] S. Yang, Y. Jiang, Z. Xu, F. Teng, Y. Hou, X. Xu, Physica B. 373 (2006) 229–232.
[15] H. Jin, Y.B. Hou, X.G. Meng, A.W. Tang, F. Teng, Chin. J. Polym. Sci. 26 (2008) 249–254.
[16] K.U. Haq, M.A. Khan, X.W. Zhang, L. Zhang, X.Y. Jiang, Z.L. Zhang, J. Non-Cryst. Solids 356 (2010) 1012–1015.
[17] G.Z. Li, N. Minami, Chem. Phys. Lett. 331 (2000) 26–30.
[18] J.H. Park, O.O. Park, J. Kim, J.W. Yu, J.K. Kim, Y.C. Kim, Curr. Appl. Phys. 4 (2004) 659–662.
[19] U.K. Mishra, J. Singh, Semiconductor Device Physics and Design. Springer, 2007.
[20] A.J. Heeger, N.S. Sariciftci, E.B. Namdas, Semiconducting and Metallic Polymers. Oxford University Press, 2010.
[21] T. Ogawa, D.C. Cho, K. Kaneko, T. Mori, T. Mizutani, Thin Solid Films 438–439 (2003) 171–176.
[22] X.D. Feng, C.J. Huang, V. Lui, R.S. Khangura, Z.H. Lu, Appl. Phys. Lett. 86 (14) (2005) 143511–143513.
[23] S. Park, D.S. Kang, D.W. Park, Y. Choe, Polym. . Korea 32 (4) (2008) 372–376.